OPEN

PRS GLOBAL OPEN

EXPERIMENTAL

Proliferating Infantile Hemangioma Tissues and Primary Cell Lines Express Markers Associated with Endothelial-to-Mesenchymal Transition

Tinte Itinteang, MBBS, PhD*
Cherise E. S. Tan, MBChB*
Bede van Schaijik, BTech (Hons)*
Reginald W. Marsh, PhD*
Paul F. Davis, PhD*
Swee T. Tan, MBBS, FRACS, PhD*†

Background: We have previously shown that the endothelium of the microvessels of infantile hemangioma (IH) exhibits a hemogenic endothelium phenotype and proposed its potential to give rise to mesenchymal stem cells, similar to the development of hematopoietic cells. This endothelial-to-mesenchymal transition (Endo-MT) process involves the acquisition of a migratory phenotype by the endothelial cells, similar to epithelial-to-mesenchymal transition that occurs during neural crest development. We hypothesized that proliferating IH expresses Endo-MT–associated proteins and investigated their expression at the mRNA, protein, and functional levels.

Methods: Immunohistochemical staining of paraffin-embedded sections of proliferating IH samples from 10 patients was undertaken to investigate the expression of the Endo-MT proteins Twist1, Twist2, Snail1, and Slug. Transcriptional analysis was performed for the same markers on proliferating IH tissues and $CD34^+$ and $CD34^-$ cells from proliferating IH-derived primary cell lines. Adipogenic and osteogenic differentiation plasticity was determined on the CD34-sorted fractions.

Results: The endothelium of the microvessels and the cells within the interstitium of proliferating IH tissues expressed Twist1, Twist2, and Slug proteins. Twist1 was also expressed on the pericyte layer of the microvessels, whereas Snail1 was not expressed. Both $CD34^+$ and $CD34^-$ populations from the IH-derived primary cell lines underwent adipogenic and osteogenic differentiation.

Conclusions: The expression of Endo-MT–associated proteins Twist1, Twist2, and Slug by both the endothelium of the microvessels and cells within the interstitium, and Twist1 on the pericyte layer of the microvessels of proliferating IH, suggest the presence of a process similar to Endo-MT. This may enable a tightly controlled primitive endothelium of proliferating IH to acquire a migratory mesenchymal phenotype with the ability to migrate away, providing a plausible explanation for the development of a fibrofatty residuum observed during involution of IH.
(Plast Reconstr Surg Glob Open 2020;7:e2598; doi: 10.1097/GOX.0000000000002598; Published online 11 February 2020.)

*From the *Gillies McIndoe Research Institute, Newtown, Wellington, New Zealand; and the †Centre for the Study & Treatment of Vascular Birthmarks, Wellington Regional Plastic, Maxillofacial and Burns Unit, Hutt Hospital, Lower Hutt, New Zealand.*

Received for publication March 4, 2019; accepted October 31, 2019.

Aspects of this work were presented at the 20th International Society for the Study of Vascular Anomalies Workshop, April 1–4, 2014, Melbourne, Australia; and the 7th Epithelial-Mesenchymal Transition International Meeting, October 11–14, 2015, Melbourne, Australia.

DOI: 10.1097/GOX.0000000000002598

INTRODUCTION

Infantile hemangioma (IH), the most common tumor of infancy, affects 4%–10% of White infants with a higher prevalence in white, female, and premature infants.[1–3] IH has traditionally been regarded a primary tumor of the microvasculature,[4] characterized by rapid postnatal growth with proliferation of endothelial cells and accumulation of myeloid hematopoietic cells.[5–7] It then undergoes spontaneous involution over the next 1–5 years as fibrofatty tissue replaces the cellular elements,[8] with on-going

Disclosure: *T.I., P.F.D., and S.T.T. are inventors of a provisional patent Treatment of Vascular Anomalies (PCT/NZ2017/050032). The authors have no financial interest to declare in relation to the content of this article.*

Related Digital Media are available in the full-text version of the article on www.PRSGlobalOpen.com.

improvement up to 10–12 years, often leaving a fibrofatty residuum containing a few mature vessels.[1–3]

The bone marrow has been proposed to be the origin of the mesenchymal stem cells (MSCs) that give rise to the adipocytes within the fibrofatty residuum of involuted IH,[9,10] whereas others have suggested the source being the endothelium of proliferating IH.[9,11]

It has been hypothesized that the endothelium of proliferating IH that consists of tightly adherent endothelial cells[12] gives rise to the MSCs, which subsequently migrate into the interstitium with eventual terminal differentiation into adipocytes, by the process of endothelial-to-mesenchymal transition (Endo-MT).[13,14] Endo-MT has been compared with the process of neural crest epithelial-to-mesenchymal transition (EMT)[13] and has been identified as a component of angiogenic sprouting during heart valve formation.[15] Intriguingly, there is, as yet, no report on the expression of mesenchymal transition–associated proteins on the endothelium of IH.

More recently, the microvessels of proliferating IH have been shown to consist of a primitive mesoderm-derived hemogenic endothelium with a neural crest phenotype,[16,17] regulated by the renin–angiotensin system with the vasoactive angiotensin II playing a crucial role.[3,18] The expression of neural crest–associated proteins p75, SOX9, and SOX10 on the endothelium of IH[16] may underscore the plasticity of the cells on the endothelium that arise from cells that migrate along predestined somite migratory routes following embolization from the placenta[19]—a concept that remains to be fully explored.

We hypothesized that the presence of a phenotypic hemogenic endothelium and the expression of neural crest–associated markers on the endothelium of proliferating IH are linked. We propose that the primitive endothelium of IH acquires an expression profile similar to an Endo-MT process which enables downstream MSCs to detach and migrate away from this phenotypic hemogenic endothelium into the interstitium. To test this hypothesis, we investigated the expression of Endo-MT–associated proteins Twist1,[20] Twist2, Snail1, and Slug (also known as Snail2),[21] in proliferating IH. Furthermore, we performed CD34 cell sorting and analyzed the expression of these aforementioned transcription factors in the $CD34^+$ and $CD34^-$ fractions of proliferating IH-derived primary cell lines and investigated their ability to undergo terminal functional mesenchymal differentiation.

METHODS

Proliferating IH Tissues

Proliferating IH tissue samples from 10 patients with a mean age of 6.5 months (range, 2–12 months) (Table 1) were sourced from the Gillies McIndoe Research Institute Tissue Bank for this study, approved by the Central Health and Disability Ethics Committee (Ref. 13/CEN/130). Written informed consent was obtained from the parents of all participants.

Table 1. Demographic Data of the Patients and the Anatomic Site of Their Proliferating Infantile Hemangioma

Patient	Sex	Age (mo)	Anatomic Site
1	M	3	Scalp
2	F	11	Forearm
3	M	2	Scalp
4	F	7	Ear
5	F	7	Scalp
6	M	4	Natal cleft
7	F	8	Scalp
8	F	12	Scalp
9	F	8	Labium
10	F	3	Mons pubis

F, female; M, male.

Immunohistochemical Staining

We have previously shown the expression of the neural crest–associated and mesenchymal-associated proteins p75, SOX9, SOX10, CD29, and vimentin on the endothelium of proliferating IH.[9,16] To demonstrate the presence of an Endo-MT process, we investigated the expression of Twist1,[20] Twist2, Snail1, and Slug,[22] transcription factors associated with the indirect induction of vimentin expression.[23]

3,3′-Diaminobenzidine (DAB) immunohistochemical (IHC) staining was performed on 4-μm-thick formalin-fixed paraffin-embedded sections of proliferating IH from 10 patients on the Leica BOND RX auto-stainer (Leica, Nussloch, Germany) as previously described,[24] using the primary antibodies for Twist1 (1:2,000; cat# ABD29; Millipore, Temecula, CA), Twist2 (1:500; cat# WHO117558; Sigma, St Louis, MO), Slug (1:75; cat# NBP2-27182; Novus Biologicals, Littleton, CO), Snail1 (1:100; cat# SAB2108482; Sigma, St Louis, MO), CD34 (ready-to-use; cat# PA0212, Leica, Newcastle, United Kingdom), and von Willebrand factor (vWF; 1:200; cat# A0082; Dako, Santa Clara, CA). All DAB IHC-stained slides were mounted in Surgipath Micromount (Leica), and all antibodies were diluted with Bond primary antibody diluent (cat# AR9352; Leica).

To further localize the expression of the Endo-MT–associated markers, immunofluorescence (IF) IHC staining was performed on proliferating IH samples from 3 patients from the cohort included in DAB IHC staining. Vectafluor Excel anti-mouse 488 (ready-to-use; cat# VEDK2488; Vector Laboratories, Burlingame, CA) and Alexa Fluor anti-rabbit 594 (1:500; cat# A21207; Life Technologies, Carlsbad, CA) were utilized to detect the combinations. All IF IHC-stained slides were mounted in VECTASHIELD Hardset mounting medium with 4′,6′-diamino-2-phenylindole (Vector Laboratories).

Human tissues showing high expression of these markers were used as positive controls: breast carcinoma for Twist1, normal liver for Twist2, and normal kidney for slug and Snail1.

Proliferating IH-Derived Primary Cell Lines

Primary cell lines derived from 6 proliferating IH samples from the 10 patients included in DAB IHC staining were sourced from the Gillies McIndoe Research Institute Tissue Bank, for analysis. These primary cell

lines were cultured in Dulbecco's Modified Eagle Medium (cat# 10569-010; Thermo Fisher Scientific, Waltham, MA) supplemented with 2% Corning Matrigel Basement Membrane Matrix (cat# 354234; Corning, NY), 10% fetal bovine serum (cat# 10091-148; Thermo Fisher Scientific), and 10,000 U penicillin–streptomycin (cat# 15140-122). The commercial cell line 3T3 (cat# CRL-1658; ATCC, Manassas, VA) was used as a positive control.

CD34 Sorting

IH-derived primary cell lines were sorted using the Dynabeads CD34 Positive Isolation Kit (cat# 11301D; Invitrogen, Carlsbad, CA) into $CD34^+$ and $CD34^-$ fractions according to the supplier's instructions.

NanoString mRNA Analysis

Six snap-frozen proliferating IH tissue samples and their matched $CD34^+$ and $CD34^-$ sorted cells from the IH-derived primary cell lines from the original cohort of 10 patients included in DAB IHC staining were used to isolate total RNA for NanoString nCounter Gene Expression Assay (NanoString Technologies, Seattle, WA). RNA was extracted from frozen tissues using RNeasy Mini Kit (Qiagen) and subjected to the NanoString nCounter gene expression assay by New Zealand Genomics Ltd (Dunedin, New Zealand). The probes for the genes encoding Twist1 (NM_000474.3), Twist2 (NM_057179.2), Snail1 (NM_003068.3), Slug (NM_005985.2), and the housekeeping gene GusB (NM_000181.1) were used. Raw data were analyzed by nSolver software (NanoString Technologies) using standard settings and were normalized against the housekeeping gene.

Statistical Analysis

Data obtained from NanoString mRNA analysis were subjected to paired *t* tests using SPSS version 24 software to determine any significant differences in the transcript expression between the markers.

Mesenchymal Differentiation Assay

The 6 $CD34^+$ and $CD34^-$ fractions of the proliferating IH-derived primary cell lines, and the 3T3 cell line (as a positive control), were plated into 8-well chamber slides (cat# 354108; Corning) at a concentration of 4×10^4 cells per well and incubated until 60%–80% confluent when the StemPro Adipogenesis Differentiation Kit (cat# A10070-01; Thermo Fisher Scientific) and StemPro Osteogenesis Differentiation Kit (cat# A10072-01; Thermo Fisher Scientific) were used for terminal mesenchymal differentiation. Differentiation media was replaced every 3–4 days according to the supplier's instructions, for up to 2 weeks. Adipogenic and osteogenic differentiation was determined by fixing and staining the cells with Oil Red O (cat# O0625; Sigma-Aldrich) and Alizarin Red (cat# A5533; Sigma-Aldrich), respectively.

Microscopy

DAB and IF IHC-stained slides were viewed and imaged using an Olympus BX53 light microscope fitted with an Olympus SC100 digital camera (Olympus, Tokyo, Japan) and with an Olympus FV1200 confocal laser-scanning microscope and processed with CellSens Dimension 1.11 software using 2-dimensional deconvolution algorithm (Olympus), respectively. Images of the Oil Red O and Alizarin Red staining were captured using a Leica DMIL LED inverted light microscope with an attached Leica DCF290 HD camera and analyzed using Leica Application Suite software (Leica, Germany).

RESULTS

IHC Staining

All tissue sections analyzed were confirmed to be IH by their expression of glucose transporter-1[25] (data not shown) on the $CD34^+$ endothelium of the microvessels surrounded by an outer concentric pericyte layer expressing smooth muscle actin.[16,17]

DAB IHC staining demonstrated expression of Twist1 (Fig. 1A), Twist2 (Fig. 1B), and Slug (Fig. 1C) but not Snail1 (Fig. 1D) in proliferating IH tissue samples on both the endothelium (Fig. 1, thick arrows) of the microvessels and cells within the interstitium (Fig. 1, arrowheads). Twist1 was also expressed on the pericyte layer (Fig. 1, thin arrows) of the microvessels.

Positive staining was demonstrated on sections of human tissues: breast carcinoma for Twist1, normal liver for Twist2, normal kidney for Slug and Snail1, respectively. Specificity of the staining was confirmed on sections of proliferating IH tissues using a matched isotype control for both mouse and rabbit primary antibodies. [see **Figure**, **Supplemental Digital Content 1,** which displays a positive control for 3,3′-diaminobezidine immunohistochemical-staining of breast carcinoma showing the expression of Twist1 (A; brown), liver for Twist2 (B; brown), kidney for Slug (C, brown) and Snail1 (D, brown). A section of proliferating infantile hemangioma tissue sample probed with a matched isotype control for mouse and rabbit primary antibodies (E, brown) confirmed specificity of the secondary antibodies. Nuclei were counterstained with hematoxylin (blue; original magnification, ×400) http://links.lww.com/PRSGO/B290.]

IF IHC staining confirmed the expression of Twist1 (Fig. 2A, red) localized to the $CD34^+$ (Fig. 2A, green) endothelium (Fig. 2A, thin arrows), the concentric pericyte layer (Fig. 2A, thick arrows), and cells within the interstitium (Fig. 2A, arrowheads). Twist2 (Fig. 2B, green) was localized to the vWF^+ (Fig. 2B, red) endothelium (Fig. 2B, thin arrows) and cells within the interstitium (Fig. 2A, arrowheads). Slug (Fig. 2C, red) was localized to the $CD34^+$ (Fig. 2C, green) endothelium (Fig. 2C, thin arrows) and cells within the interstitium (Fig. 2C, arrowheads). Snail1 (Fig. 2D, green) was expressed by very few cells within the interstitium, away from the microvessels.

Split images of IF IHC staining presented in Figure 2 are shown in Supplemental Digital Content 2. [See

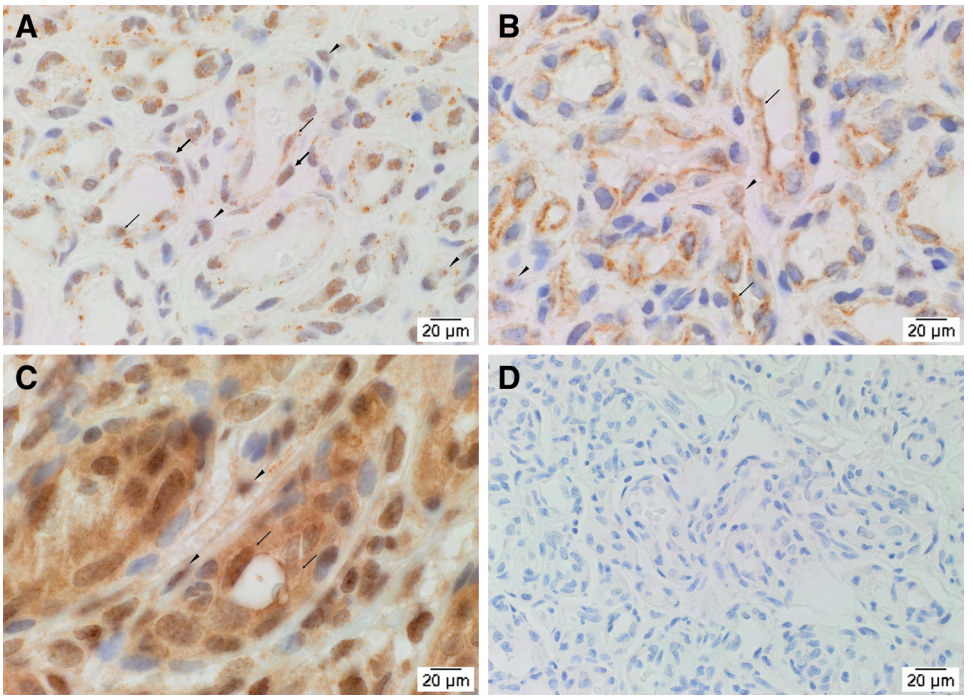

Fig. 1. Representative 3,3′-diaminobenzidine immunohistochemical staining on proliferating infantile hemangioma tissue samples demonstrating the expression of Twist1 (A, brown), Twist2 (B, brown), and Slug (C, brown) but not Snail1 (D, brown), on the endothelium of the microvessels (thin arrows) and the cells within the interstitium (arrowheads). Twist1 was also expressed on the pericyte layer (thick arrows) of the microvessels. Nuclei were counterstained with hematoxylin (blue). Original magnification: ×400.

Figure, Supplemental Digital Content 2, which displays split immunofluorescence immunohistochemical-stained images of Twist1 (A, red) and CD34 (B, green); vWF (C, red) and Twist2 (D, green); Slug (E, red) and CD34 (F, green), Slug (G, red) and Snail1 (H, green). A negative control which demonstrated minimal staining confirming specificity of the primary antibodies (I). Cell nuclei were counterstained with 4′,6′-diamidino-2-phenylindole (blue). Original magnification: 400x. http://links.lww.com/PRSGO/B291.]

NanoString mRNA Analysis

NanoString mRNA analysis confirmed transcript expression of Twist1, Twist2, Snail1, and Slug, relative to the housekeeping gene GusB, in both the snap-frozen IH tissue samples and the $CD34^+$ and $CD34^-$ cell fractions of the IH-derived primary cell lines (Fig. 3). Statistical analysis showed a significantly greater expression of Twist2 compared with Twist1 ($P < 0.05$) and Slug compared with Snail1 ($P < 0.01$) that in the snap-frozen IH tissue sample. A significant increase in expression was also observed between Twist2 and Twist 1 and between Slug and Snail1 in both the $CD34^+$ ($P < 0.01$) and $CD34^-$ ($P < 0.01$) proliferating IH-derived primary cell lines.

MSC Differentiation

Following the addition of the differentiation supplements, staining of lipid droplets by Oil Red O was observed in all 6 $CD34^+$ (Fig. 4A, red) and 6 $CD34^-$ (Fig. 4B, red) fractions, as was also observed in the 3T3 positive control (Fig. 4C, red), and staining of calcium deposits by Alizarin Red was observed in all 6 $CD34^+$ (Fig. 4D, red) fraction and $CD34^-$ (Fig. 4E, red) fraction, as was see in the 3T3 positive control (Fig. 4F, red), confirming the adipogenic and osteogenic differentiation capability of proliferating IH. Cells grown in non-supplemented media were used as negative controls which show minimal staining [**See Figure, Supplemental Digital Content 3**, which displays negative control images of proliferating IH-derived primary cell lines grown in non-supplemented media and stained with Oil Red O (A) and Alizarin Red (B). Original magnification: ×400, http://links.lww.com/PRSGO/B292.]

DISCUSSION

There is growing evidence of the involvement of stem cells in the biology of IH with recent data supporting a placental chorionic villous mesenchymal core cell origin.[19] The concept that IH is a developmental anomaly due to aberrant proliferation and differentiation of a phenotypic hemogenic endothelium[17] derived from a primitive mesoderm with a neural crest phenotype[16] underscores the understanding of the biology of IH. We have further shown plasticity of the IH phenotypic hemogenic endothelium-derived cells to undergo both mesenchymal[9] and hematopoietic[5,19] differentiation

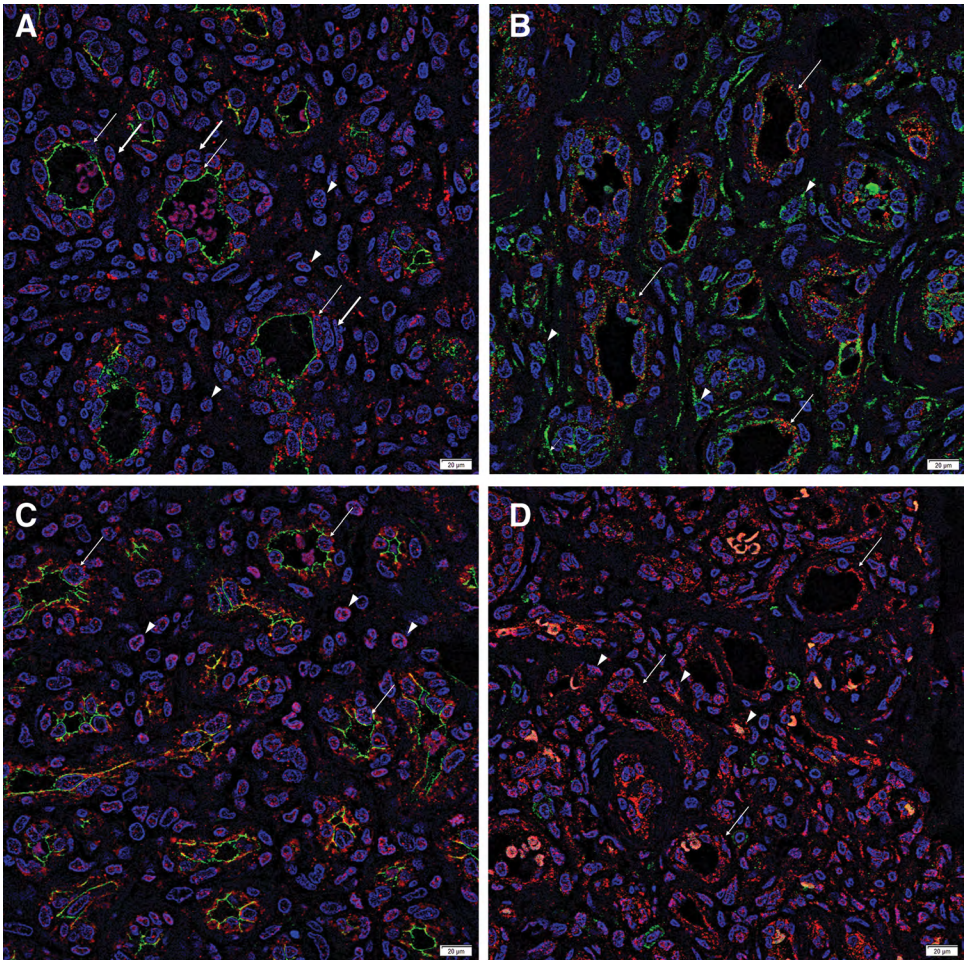

Fig. 2. Representative immunofluorescence immunohistochemical staining on proliferating infantile hemangioma tissue samples demonstrating the expression of Twist1 (A, red) localized to the $CD34^+$ (green) endothelium (thin arrows), the concentric pericyte layer (thick arrows), and the cells within the interstitium (arrowheads). Twist2 (B, green) was localized to the vWF^+ (red) endothelium (thin arrows) and cells within the interstitium (arrowheads). Slug (C, red) was localized to the $CD34^+$ (green) endothelium (thin arrows) and cells within the interstitium (arrowheads). Snail1 (D, green) was localized to few cells within the interstitium that also expressed Slug (red) which was widely expressed by the endothelium (thin arrows) and other cells within the interstitium (arrowheads). All slides were counterstained with 4′, 6′-diamino-2-phenylindole (blue). Original magnification: ×400.

with critical regulation by the renin–angiotensin system.[3]

The presence of an MSC/mesenchymal progenitor cell population within IH has been observed, and these cells are presumed to be derived from adjacent niches.[10] However, recent reports have demonstrated expression of mesenchymal-associated proteins, vimentin, preadipocyte factor-1, and CD29, on the endothelium of proliferating IH,[9] implying an endo-mesenchymal phenotype which suggests the origin of the MSC/mesenchymal progenitor cell population is the primitive endothelium of IH.[9]

The shedding of cells from a tightly regulated endothelium, consisting of tightly bound vascular endothelial (VE)-cadherin junctions on the endothelium of proliferating IH,[12] involves the detachment of cells from the endothelium in a process known as Endo-MT,[13] analogous to the process of neural crest EMT.[22] Endo-MT is typically observed during fetal cardiac development, critically in the development of the mesenchymal heart cushion cells from the cardiac endocardial cells.[26,27] We investigated the expression of Endo-MT–associated proteins within proliferating IH to demonstrate these biological parallels with the established concept of neural crest EMT and IH development.

The collective expression of Twist1, Twist2, and Slug demonstrated in this study by both the IH tissue samples and cells derived from proliferating IH, coupled with the ability for both the endothelial and non-endothelial populations to undergo mesenchymal differentiation support the Endo-MT concept.[22,27–30] Interestingly, the putative presence of an MSC-phenotypic precursor in

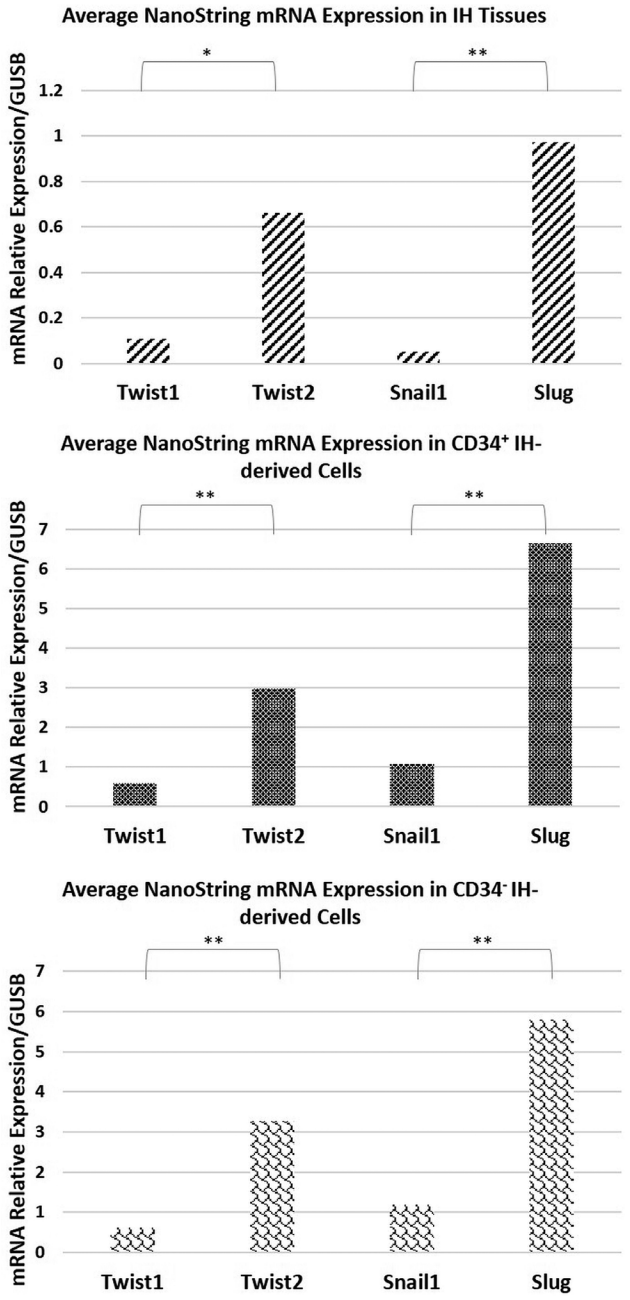

Fig. 3. NanoString mRNA analysis confirming transcript expression of Twist1, Twist2, Snail1, and Slug in proliferating infantile hemangioma (IH) tissue samples, and both the $CD34^+$ and $CD34^-$ proliferating IH-derived primary cell lines, relative to the housekeeping gene GusB. Levels of statistical significance are shown above the graphs (*$P < 0.05$; **$P < 0.01$).

both the endothelial and non-endothelial populations suggests the putative presence of 2 separate population of stem cells endowed with mesenchymal transition plasticity. This is supported by the terminal mesenchymal differentiation capacity of both the $CD34^+$ and $CD34^-$ populations, similar to the findings of Huang et al.[11] Snail1 is expressed on a few cells within the interstitium which are morphologically similar to mast cells which have been shown to express a primitive phenotype.[5] The significance of this requires further investigation. The minimal mRNA expression of Snail1 by the IH tissues and IH-derived primary cell lines suggests a lesser role for this marker in the Endo-MT process in IH. Corroborating our findings is the demonstration of the role of activated Notch 1 and Notch 4 receptors during Endo-MT and the presence of these receptors and their ligand, Jagged 1, on the endothelium of IH.[31] The greater expression of Slug and Twist2 compared with Snail1 and Twist1, respectively, may indicate a level of hierarchical expression of these markers, which may provide a platform for further research.

To the best of our knowledge, this is the first report demonstrating the expression of Endo-MT–associated proteins on a phenotypic hemogenic endothelium of IH. This may account for the ability of downstream MSCs to bud off and detach from this primitive endothelium and then migrate away. This novel concept of a "delaminating endothelium" may potentially explain the delamination phenomenon of downstream progenitors by the process of Endo-MT,[32] although this requires further investigation. This is consistent with the observation of the ability of IH-derived stem cells to form human blood vessels in immunodeficient mice,[33] suggesting the capability of IH cells to "bud off" via an Endo-MT process.

Recent studies have shown an endothelial origin of hematopoiesis, underscoring the concept of a hemogenic endothelium, with live imaging confirming a hematopoietic cells "budding" off the endothelium and migrating away.[34] The novel findings presented in this report offer some interesting insights into the cellular dynamics that govern this crucial transition state of a delaminating endothelium suggesting the presence of an Endo-MT–like process in the pathogenesis of IH. We propose that this delaminating endothelium has the potential to give rise to the EPCs that are shed into the circulation and potentially to the MSCs in the surrounding interstitium typically seen during the Endo-MT that occurs during early cardiac development.[26] The findings of this study provide a plausible explanation for the development of a fibrofatty residuum observed during involution of IH.

Swee T. Tan, MBBS, FRACS, PhD
Gillies McIndoe Research Institute
PO Box 7184, Newtown 6242
Wellington, New Zealand
E-mail: swee.tan@gmri.org.nz

ACKNOWLEDGMENTS

We thank Ms. Liz Jones and Dr. Helen Brasch, and Mr. Matthew Munro and Ms. Kirsty Myall of the Gillies McIndoe Research Institute for their assistance in immunohistochemical staining and for performing preliminary cell culture work, respectively.

Statement of Conformity: This study was carried out with the approval of the Central Health and Disability Ethics Committee (Ref. 13/NTB/155) with written informed consent from all subjects in accordance with the Declaration of Helsinki. Written informed consent was obtained from all participants.

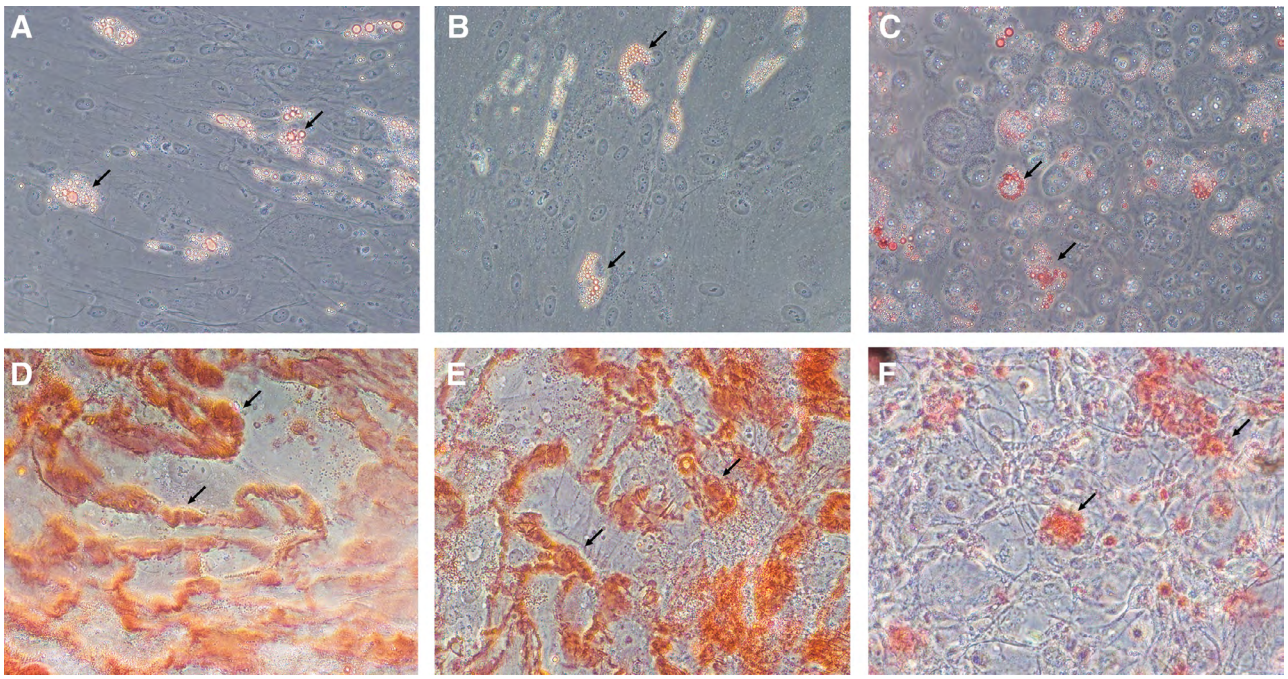

Fig. 4. Mesenchymal differentiation assays of proliferating infantile hemangioma–derived primary cell lines demonstrating lipid droplets stained with Oil Red O in $CD34^+$ (A, red, arrows) and $CD34^-$ (B, red, arrows) cellular fractions for adipogenesis relative to the 3T3 positive control (C, red, arrows), and calcium deposits stained with Alizarin Red in $CD34^+$ (D, red, arrows) and $CD34^-$ (E, red, arrows) cellular fractions for osteogenesis relative to the 3T3 positive control (F, red, arrows). Original magnification: ×400.

REFERENCES

1. Amrock SM, Weitzman M. Diverging racial trends in neonatal infantile hemangioma diagnoses, 1979-2006. *Pediatr Dermatol.* 2013;30:493–494.
2. Hoornweg MJ, Smeulders MJ, Ubbink DT, et al. The prevalence and risk factors of infantile haemangiomas: a case-control study in the Dutch population. *Paediatr Perinat Epidemiol.* 2012;26:156–162.
3. Tan ST, Itinteang T, Leadbitter P. Low-dose propranolol for infantile haemangioma. *J Plast Reconstr Aesthet Surg.* 2011;64: 292–299.
4. Mulliken JB, Glowacki J. Hemangiomas and vascular malformations in infants and children: a classification based on endothelial characteristics. *Plast Reconstr Surg.* 1982;69:412–422.
5. Itinteang T, Tan ST, Jia J, et al. Mast cells in infantile haemangioma possess a primitive myeloid phenotype. *J Clin Pathol.* 2013;66:597–600.
6. Ritter MR, Reinisch J, Friedlander SF, et al. Myeloid cells in infantile hemangioma. *Am J Pathol.* 2006;168:621–628.
7. Tan ST, Wallis RA, He Y, et al. Mast cells and hemangioma. *Plast Reconstr Surg.* 2004;113:999–1011.
8. Itinteang T, Brasch HD, Tan ST, et al. Expression of components of the renin-angiotensin system in proliferating infantile haemangioma may account for the propranolol-induced accelerated involution. *J Plast Reconstr Aesthet Surg.* 2011;64:759–765.
9. Itinteang T, Vishvanath A, Day DJ, et al. Mesenchymal stem cells in infantile haemangioma. *J Clin Pathol.* 2011;64:232–236.
10. Yu Y, Fuhr J, Boye E, et al. Mesenchymal stem cells and adipogenesis in hemangioma involution. *Stem Cells.* 2006;24:1605–1612.
11. Huang L, Nakayama H, Klagsbrun M, et al. Glucose transporter 1-positive endothelial cells in infantile hemangioma exhibit features of facultative stem cells. *Stem Cells.* 2015;33:133–145.
12. Martìn-Padura I, De Castellarnau C, Uccini S, et al. Expression of VE (vascular endothelial)-cadherin and other endothelial-specific markers in haemangiomas. *J Pathol.* 1995;175:51–57.
13. Kovacic JC, Mercader N, Torres M, et al. Epithelial-to-mesenchymal and endothelial-to-mesenchymal transition: from cardiovascular development to disease. *Circulation.* 2012;125:1795–1808.
14. Li Y, Lui KO, Zhou B. Reassessing endothelial-to-mesenchymal transition in cardiovascular diseases. *Nat Rev Cardiol.* 2018;15:445–456.
15. Welch-Reardon KM, Wu N, Hughes CC. A role for partial endothelial-mesenchymal transitions in angiogenesis? *Arterioscler Thromb Vasc Biol.* 2015;35:303–308.
16. Itinteang T, Tan ST, Brasch H, et al. Primitive mesodermal cells with a neural crest stem cell phenotype predominate proliferating infantile haemangioma. *J Clin Pathol.* 2010;63:771–776.
17. Itinteang T, Tan ST, Brasch H, et al. Haemogenic endothelium in infantile haemangioma. *J Clin Pathol.* 2010;63:982–986.
18. Tan ST, Itinteang T, Day DJ, et al. Treatment of infantile haemangioma with captopril. *Br J Dermatol.* 2012;167:619–624.
19. Itinteang T, Tan ST, Brasch HD, et al. Primitive erythropoiesis in infantile haemangioma. *Br J Dermatol.* 2011;164:1097–1100.
20. Yang J, Mani SA, Donaher JL, et al. Twist, a master regulator of morphogenesis, plays an essential role in tumor metastasis. *Cell.* 2004;117:927–939.
21. Fenouille N, Tichet M, Dufies M, et al. The epithelial-mesenchymal transition (EMT) regulatory factor SLUG (SNAI2) is a downstream target of SPARC and AKT in promoting melanoma cell invasion. *Plos One.* 2012;7:e40378.
22. Kalluri R, Weinberg RA. The basics of epithelial-mesenchymal transition. *J Clin Invest.* 2009;119:1420–1428.
23. Gao H, Zhang J, Liu T, et al. Rapamycin prevents endothelial cell migration by inhibiting the endothelial-to-mesenchymal transition and matrix metalloproteinase-2 and -9: an *in vitro* study. *Mol Vis.* 2011;17:3406–3414.
24. Tan EM, Blackwell MG, Dunne JC, et al. Neuropeptide Y receptor 1 is expressed by B and T lymphocytes and mast cells in infantile haemangiomas. *Acta Paediatr.* 2017;106:292–297.

25. North PE, Waner M, Mizeracki A, et al. GLUT1: a newly discovered immunohistochemical marker for juvenile hemangiomas. *Hum Pathol.* 2000;31:11–22.
26. Combs MD, Yutzey KE. Heart valve development: regulatory networks in development and disease. *Circ Res.* 2009;105:408–421.
27. Arciniegas E, Frid MG, Douglas IS, et al. Perspectives on endothelial-to-mesenchymal transition: potential contribution to vascular remodeling in chronic pulmonary hypertension. *Am J Physiol Lung Cell Mol Physiol.* 2007;293:L1–L8.
28. Acloque H, Adams MS, Fishwick K, et al. Epithelial-mesenchymal transitions: the importance of changing cell state in development and disease. *J Clin Invest.* 2009;119:1438–1449.
29. Huang B, Pi L, Chen C, et al. WT1 and pax2 re-expression is required for epithelial-mesenchymal transition in 5/6 nephrectomized rats and cultured kidney tubular epithelial cells. *Cells Tissues Organs.* 2012;195:296–312.
30. Lee JM, Dedhar S, Kalluri R, et al. The epithelial-mesenchymal transition: new insights in signaling, development, and disease. *J Cell Biol.* 2006;172:973–981.
31. Wu JK, Kitajewski JK. A potential role for notch signaling in the pathogenesis and regulation of hemangiomas. *J Craniofac Surg.* 2009;20 Suppl 1:698–702.
32. Yue R, Li H, Liu H, et al. Thrombin receptor regulates hematopoiesis and endothelial-to-hematopoietic transition. *Dev Cell.* 2012;22:1092–1100.
33. Khan ZA, Boscolo E, Picard A, et al. Multipotential stem cells recapitulate human infantile hemangioma in immunodeficient mice. *J Clin Invest.* 2008;118:2592–2599.
34. Eilken HM, Nishikawa S, Schroeder T. Continuous single-cell imaging of blood generation from haemogenic endothelium. *Nature.* 2009;457:896–900.